Megakaryocyte endomitosis is a failure of late cytokinesis related to defects in the contractile ring and Rho/Rock signaling

Larissa Lordier,[1-3] Abdelali Jalil,[3] Fréderic Aurade,[1-4] Fréderic Larbret,[1,3] Jérôme Larghero,[5] Najet Debili,[1-3] William Vainchenker,[1-3] and Yunhua Chang[1-3]

[1]Inserm, U790, Villejuif; [2]Université Paris XI, Villejuif; [3]Institut Gustave Roussy, IFR54, Villejuif; [4]Centre National de la Recherche Scientifique (CNRS), UPMC University Paris 06, Unité Mixte de Recherche (UMRS) 787, Paris; and [5]Inserm, EMI00-03, Laboratoire de Biologie Cellulaire Hématopoïétique, Hôpital Saint-Louis, Paris, France

Megakaryocyte (MK) is the naturally polyploid cell that gives rise to platelets. Polyploidization occurs by endomitosis, which was a process considered to be an incomplete mitosis aborted in anaphase. Here, we used time-lapse confocal video microscopy to visualize the endomitotic process of primary human megakaryocytes. Our results show that the switch from mitosis to endomitosis corresponds to a late failure of cytokinesis accompa-nied by a backward movement of the 2 daughter cells. No abnormality was observed in the central spindle of endomi-totic MKs. A furrow formation was present, but the contractile ring was abnormal because accumulation of nonmuscle myo-sin IIA was lacking. In addition, a defect in cell elongation was observed in dipolar endomitotic MKs during telophase. RhoA and F-actin were partially concentrated at the site of furrowing. Inhibition of the Rho/Rock pathway caused the disappear-ance of F-actin at midzone and increased MK ploidy level. This inhibition was asso-ciated with a more pronounced defect in furrow formation as well as in spindle elongation. Our results suggest that the late failure of cytokinesis responsible for the endomitotic process is related to a partial defect in the Rho/Rock pathway activation. (Blood. 2008;112:3164-3174)

Introduction

Megakaryocytes (MKs) are the hematopoietic cells that give rise to platelets by fragmentation of their cytoplasm through pseudopodial formations, called proplatelets. During their differentiation, MKs become polyploid by a unique process called endomitosis. Recent studies have shown that MK endomitosis is an incomplete multipo-lar mitosis characterized by a failure in both nuclear (karyokinesis) and cytoplasmic division (cytokinesis) producing a cell that contains a unique multilobulated nucleus. Polyploidization (up to 128N) is achieved by successive cycles of endomitosis. Several studies have described the endomitotic stages up to anaphase and these data have led to the assumption that endomitosis corre-sponded to a late failure of mitosis during anaphase without cleavage furrow formation and spindle elongation.[1,2] However, the late endomitotic stages beyond anaphase have not yet been observed in detail and the molecular mechanisms controlling the switch from a mitotic to an endomitotic process are still unknown.

During mitosis, the transition from metaphase to anaphase is characterized by the formation of a network of antiparallel microtubules between the separating chromosomes, called the midzone.[3,4] The midzone is required for maintenance of the overall spindle architecture, for spindle elongation and cleavage furrow positioning. Many proteins essential for cytokinesis are localized to the midzone. It was believed that the late mitotic abnormalities in endomitotic MKs were associated with defects in the expression or function of 1 or more midzone components. However, although controversial, endomitotic MKs appear to form an intact midzone structure with the presence of proteins such as Aurora B, MKLP2 (mitotic kinesin-like protein 2), and MgcRacGAP that play an essential role in regulating midzone formation and cytokinesis.[5] Thus, these data suggested the failure in mitosis had to take place at stages later than anaphase, as reported in a recent work.[6]

Small GTPases from the Rho family (eg, RhoA, Rac1, and Cdc42) are required for many cellular functions such as actin reorganization, transcriptional activation, cell mobility, and cytoki-nesis.[7] During mitosis, activated RhoA accumulates in the cleavage furrow promoting the activation of several effectors, including Rho kinase (Rock), citron kinase, LIM kinase, and mDia/formins. Activation of the RhoA pathway leads to the assembly and constriction of the actomyosin ring, ingression of the cleavage furrow, and completion of cytokinesis.[4,8-10] In addition, Rho/Rock may also control the cell elongation that occurs in anaphase B.[11] Because of the importance of RhoA in late phases of mitosis, a defect in its signaling may be involved in the MK endomitotic process. In favor of this hypothesis, a previous study established that there is no accumulation of RhoA or actin at the cleavage furrow in anaphase during endomitosis.[5]

Using real-time confocal video microscopy, we demonstrated that endomitosis corresponds to a late failure of cytokinesis accompanied by a backward movement of the daughter cells. The phenomenon of reversal of cytokinesis was associated with a partial accumulation of RhoA and F-actin at the midzone. In addition, myosin II was not recruited in the contractile ring in a fraction of cell at the 2N and 4N transition, suggesting that it could play an important role in cytokinesis failure. Inhibition of RhoA and Rock accentuated the defects in contractile ring and furrow formation, as well as in spindle elongation. These data indicate that

endomitosis is associated with a deficiency in contractile ring formation and spindle elongation that may be associated with a partial defect in Rho/Rock signaling.

Methods

In vitro culture of MKs derived from human CD34$^+$ cells in liquid serum-free medium

CD34$^+$ cells were obtained, in agreement with our institutional ethics committee (Assistance Publique des Hôpitaux de Paris) and in accordance with the Declaration of Helsinki, from the bone marrow of healthy patients undergoing hip surgery. CD34$^+$ cells were isolated using an immunomagnetic cell sorting system (AutoMacs; Miltenyi Biotec, Paris, France) with "Possel d2" protocol. Purity evaluated by flow cytometry was more than 98%. CD34$^+$ cells were cultured in serum-free medium in the presence of recombinant human thrombopoietin (rhTPO; 10 ng/mL; Kirin Brewery, Tokyo, Japan) for inducing MK differentiation. Ingredients used to prepare the serum-free medium were as previously described.[12]

Lentiviral constructs

The EF1a-H2BGFP fragment was excised and subcloned into an HIV-derived lentiviral vector (pRRLsin-PGK-eGFP-WPRE; Généthon, Evry, France) in place of the PGK-eGFP sequence. The shRNA cloning and lentiviral construction are described in Document S1 (available on the *Blood* website; see the Supplemental Materials link at the top of the online article).[13,14]

Lentivirus production

Lentivirus stocks were prepared as previously described.[15] The lentivirus stocks containing approximately 10^9 infectious particles/mL were aliquoted and kept frozen at −80°C.

Cell transduction by lentivirus

Isolated CD34$^+$ cells were cultured for 4 days with rhTPO (10 ng/mL). Lentiviral particles were added at a concentration of 10^7 infectious particles/10^5 cells for 12 hours followed by a second transduction. Cells were continuously cultured in the presence of rhTPO.

Retroviral plasmid construction, retrovirus production, and cell infection

Construction of the Migr-RhoAN19-GFP retroviral plasmid and production of retrovirus were performed as previously described.[16] The details of cell infection are described in Document S1.

Electroporation

TatC3 (10 μg/mL) and muted TatC3 (10 μg/mL) were delivered into MKs by the Amaxa electroporation system (Amaxa, Gaithersburg, MD).

Measurement of ploidy

Hoechst 33 342 (10 μg/mL; Sigma-Aldrich, St Quentin Fallavier, France) was added in the medium of cultured MKs for 2 hours at 37°C. Cells were centrifuged and then stained with the anti-CD41 APC and anti-CD42 PE MoAbs (Pharmingen, Lyon, France) for 30 minutes at 4°C. The ploidy was measured in the CD41$^+$/CD42$^+$ cell population when chemical inhibitors were tested and in the CD41$^+$/CD42$^+$/GFP$^+$ population after lentiviral infection by an LSRII (Becton Dickinson, Le Pont de Claix, France) flow cytometer equipped with 3 lasers (360 nM, 480 nM, and 560 nM excitation). The mean ploidy was calculated by the following formula:

(2N × number of cells at 2N ploidy) + (4N × number of cells at 4N ploidy) + (. . .) + (64N × number of cells at 64N ploidy) / total number of cells

Immunofluorescence

Fixation and immunofluorescence were performed on CD41$^+$ MKs sorted at day 6 and cultured overnight before the experiments as described previously.[16] The following antibodies were used: rabbit anti-PRC1 (dilution: 1:100; Santa Cruz Biotechnology, Santa Cruz, CA), rabbit anti-nonmuscle Myosin IIA (dilution:1:100; Sigma-Aldrich), Phalloidin-TRITC (dilution:1:800; Dako, Trappes, France), rabbit anti-α tubulin (dilution: 1:100; ABR, Golden, CO), rabbit anti-MKLP (dilution: 1:100; Abcam, Paris, France), mouse anti-α tubulin and mouse anti-β tubulin MoAbs (dilution:1:200; Sigma-Aldrich). For mouse anti-RhoA (dilution:1:100; Santa Cruz Biotechnology), the CD41$^+$ MKs were fixed with ice-cold 10% trichloroacetic acid (TCA) for 15 minutes and then washed with PBS containing 30 mM glycine 3 times before immunofluorescence. The appropriate secondary antibodies used were conjugated with Alexa 488 or Alexa 546 (dilution: 1:200; Molecular Probes-Invitrogen, Cergy-Pontoise, France). TOTO-3 iodide (dilution: 1:1000; Molecular Probes) was applied for nucleus staining. Cells were examined under a Zeiss LSM 510 laser scanning microscope (Carl Zeiss, Le Pecq, France) with a 63×/1.4 numeric aperture (NA) oil objective.

Live cell imaging by confocal video microscopy

Isolated CD34$^+$ cells were cultured for 3 days in serum-free medium in the presence of rhTPO (10 ng/mL) and then infected with the H2B-GFP lentivirus as described in "Cell transduction by lentivirus." After infection, cells were cultivated in serum-free medium in the presence of rhTPO for 48 to 72 hours and then stained with CellTracker Red according to the protocol of the product datasheet (Invitrogen) and CD41APC moAb. Cells were subsequently seeded in glass bottom culture dish (MatTek, Ashland, MA).

Cells were imaged under a Zeiss LSM 510 laser scanning microscope using a 63×/1.4 NA oil objective at 37°C with 5% CO_2. A more detailed description of the process is presented in Document S1.

Western blot analysis

Western blot analysis was performed as described previously[16] with the following antibodies: rabbit anti–Rock I (Santa Cruz Biotechnology) and rat anti–Hsc70 (Santa Cruz Biotechnology) and blots were quantified by the ImageJ program (http://rsb.info.nih.gov/ij).

Real-time quantitative RT-PCR

Real-time reverse transcription–polymerase chain reaction (RT-PCR) was performed as previously described.[17] Primers for Rock I mRNA were as follows: sense: 5′-GCTGAACGAAGAGACAGAGGTCAT-3′; antisense: 5′-GCTTCACCTCCTCTTGTAAAGATGTA-3′; the internal probe: 5′-CTGAGATGATTGGAGACCTTCAAGCTCGA-3′.

Results

Polyploidization in MKs results from a late reversal of cytokinesis

MKs undergo endomitosis to increase their ploidy during megakaryocytopoiesis. Here, time-lapse microscopy was used to visualize MK endomitosis on living primary human MKs. To precisely follow the endomitotic process, MKs were transduced with a lentiviral vector expressing Histone 2B fused to GFP (H2B-GFP) and then images were taken every 3 or 5 minutes.

In a first set of experiments, we examined MKs defined as CD41APC positive cells at the 2N to 4N transition. As illustrated in Figure 1A and also in Video S1, endomitosis proceeded exactly as a normal mitosis until anaphase. A cell elongation with 2 separated nuclear masses was accompanied with the formation of a cleavage furrow. The 2 daughter cells reached a point where they were
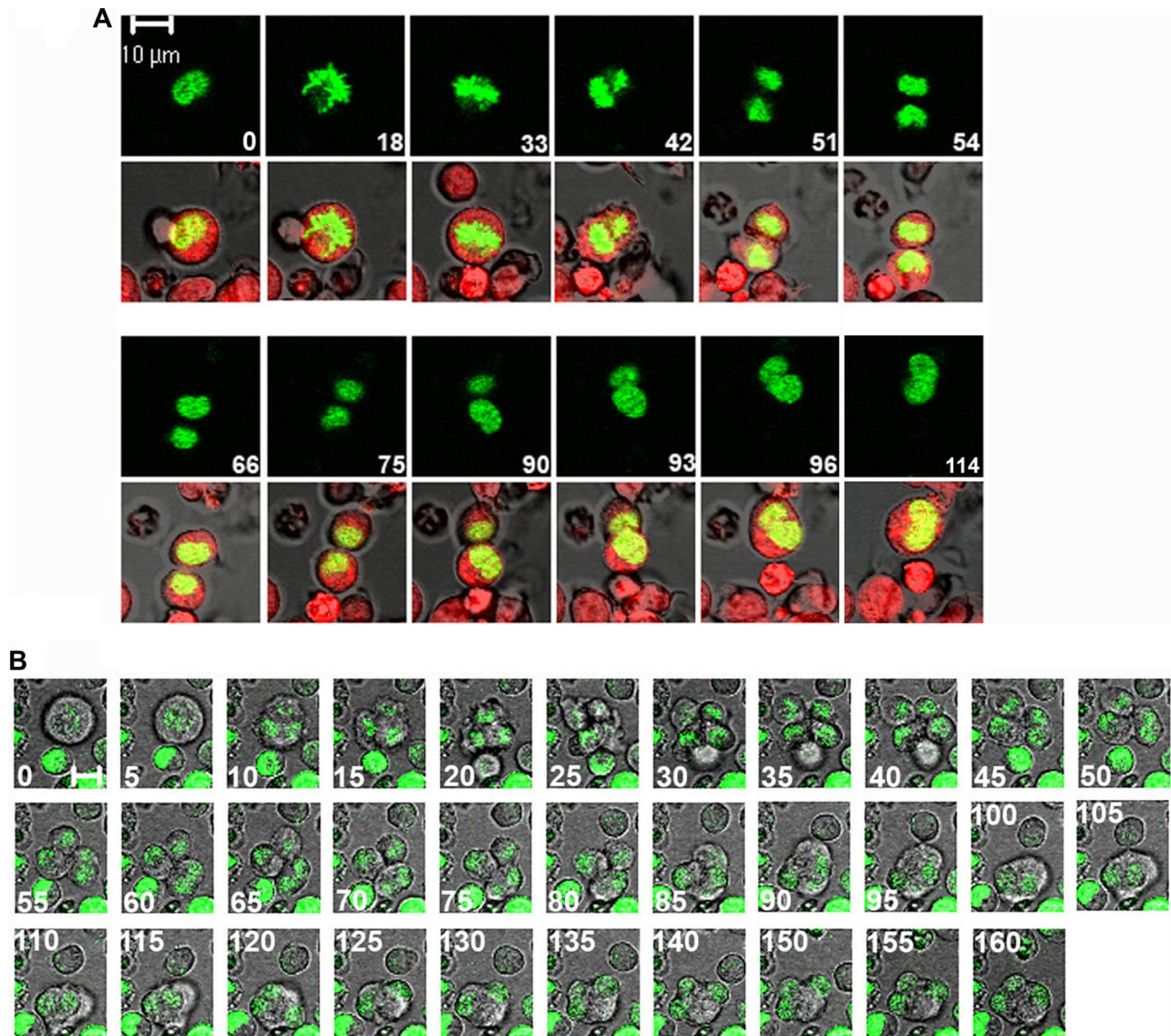
Figure 1. Polyploidization in MK results from a late reversal of cytokinesis. Primary cultured MKs from human bone marrow were transduced with a plasmid encoding H2B-GFP. Time-lapse images were obtained by confocal video microscopy. Time relative to the first image is indicated in minutes on each photograph. Bars represent 10 μm. (A) A mitosis/endomitosis transition. The cell was stained with CellTracker Orange and serial images were obtained at 3 minutes interval. Endomitosis proceeded exactly as a mitosis until the late telophase when the 2 nuclear masses are separated and the 2 daughter cells are connected by a cytoplasm bridge (images 54,66). Thereafter, the 2 daughter cells moved backward toward each other (images 75-96) and reassembled into 1 single cell with only 1 nuclear mass (image 114). (B) An endomitosis in a polyploid MK. Serial images were obtained at 5-minute intervals. Endomitosis proceeded as a mitosis but DNA was scattered at 4 poles until the end of cytokinesis (images 0-40). The 4 daughter cells remained connected (images 30,35,40). Then the incipient daughter cells moved backward and are reunified 2-by-2 (images 45-85). These time-lapse images are available in Videos S1 and S2.

connected only by a cytoplasm bridge (Figure 1A, images 54-66). However, the 2 cells failed to separate and stayed almost 30 minutes at this stage. Thereafter, the 2 daughter cells moved backward (Figure 1A, images 75-93) and finally reassembled into one single cell (Figure 1A, images 96-99). Thus, the 2N to 4N endomitotic MKs failed to undergo abcission. We filmed 11 instances of endomitosis of MKs at the 2N to 4N transition in 8 independent experiments and observed a late reversal of cytokinesis process in all of them. At the same time, we also filmed 24 diploid MKs undergoing mitosis where completion of cytokinesis and separation of the 2 daughter cells were always seen (data not shown).

Whereas we observed a failure of cytokinesis in all 2N to 4N endomitotic MKs, nuclear division did not always fail. Among 4N interphase MKs, a fraction of the cells presented a single nucleus (bilobulated or monolobulated), another fraction presented 2 separated nuclei, and the third fraction presented 2 side-by-side nuclei,

but it remained difficult to assume that they were completely separated (Figure S1). The percentage of each fraction varied among experiments. In 3 independent experiments (more than 300 cells were counted in each experiment), the MKs that presented 2 separated nuclei could vary from 19.5% to 46.6%, and the MKs with 2 side-by-side nuclei from 15% to 27%.

The internuclear distance at the end of telophase was evaluated by the length separating the center of each nuclear mass. The average distance in endomitotic dipolar cells was 8.91 μm plus or minus 2.13 (n = 11), and this distance was 10.54 μm plus or minus 1.73 (n = 24) for mitotic cells, indicating an approximately 16% reduction in cell elongation during endomitosis compared with mitosis ($P < .05$; see Figure 7C).

Next, we examined the endomitotic sequence in CD41 APC positive cells at the 4N to 8N transition and at higher ploidy levels. Endomitosis in polyploid MKs proceeded similarly as observed in

2N cells (Figure 1B; see also Video S2), except that during cell elongation from late anaphase to late telophase, 4 daughter cells were formed that remained linked by a cytoplasm connection, exactly like a flower with 4 petals (Figure 1B, images 30-40). The backward movement occurred asynchronously in the 2 pairs of daughter cells. At first, 2 incipient daughter cells reunified leading to a transient presence of 3 daughter cells (Figure 1B, images 45-80). Thereafter, the endomitosis finished by joining the 2 polyploid daughter cells together. Sixteen multipolar endomitotic MKs were filmed in 9 independent experiments. A late reversal of cytokinesis was observed in 13 polyploid endomitotic MKs. Two polyploid endomitotic MKs showed attenuated furrow ingression compared with dipolar endomitotic MK; a similar phenomenon was observed by Geddis et al in murine polyploid endomitotic MK (Figure S2A).[6] Another one presented a complete absence of furrowing (Figure S2B).

The defect in furrowing was mostly seen in endomitotic MKs with a high ploidy (> 8N). We also observed a polyploid endomitotic MK presenting 8 petals at the end of telophase, which reunified to form 1 cell (Video S4 and Figure S3). This reversal of cytokinesis was not due to lentiviral toxicity because a similar phenomenon was observed under bright field examination when H2B-GFP was not transduced (data not shown). These results indicate that the mechanism responsible for MK polyploidization is not a mitotic abort in anaphase, but a late reversal of cytokinesis. We thus focalized our study on the cytokinetic machinery.

Core components of the central spindle are normally localized in the midzone during anaphase and in the midbody during telophase in endomitosis

During anaphase, one of the most remarkable events is the formation of a central spindle, a set of microtubule-based structures.[3] Many core components of the central spindle are required for cytokinesis. These include the chromosome passenger proteins, Survivin and Aurora B,[18] the microtubule-associated protein, PRC1 (protein regulating cytokinesis 1),[19] a subunit of the centralspindlin complex, MKLP1 (mitotic kinesin-like protein-1), and microtubules. We examined the distribution of PRC1, Survivin, Aurora B, MKLP1, and tubulin in the central spindle during CD41$^+$ MK endomitosis by immunofluorescence. We observed that these proteins had an appropriate localization and we show herein the distribution of PRC1 and tubulin as an example. During anaphase, microtubules congregated midway between the 2 poles of the central spindle, while PRC1 accumulated in the midzone and colocalized with the central spindle (Figure 2A). During telophase, the central spindle was highly concentrated, forming 1 intercellular bridge. The anti-α and anti-β tubulin antibodies marked the edges of the intercellular bridge, but not the midbody itself. PRC1 was present in the center of the central spindle (Figure 2B). Altogether, these observations indicate that the distribution of PRC1 and microtubules is similar in an endomitosis and a mitosis.

Myosin II is not recruited in the contractile ring of most mitotic and endomitotic MKs

During anaphase, the actomyosin contractile ring formation is another principal cytokinetic structure. The contractile ring generally creates a cleavage furrow between the 2 daughter cells and plays a crucial role in cell abscission. To examine if the contractile ring was correctly formed in endomitotic CD41$^+$ MKs, we investigated the accumulation of its 2 major components, nonmuscle myosin IIA and actin filaments (F-actin).
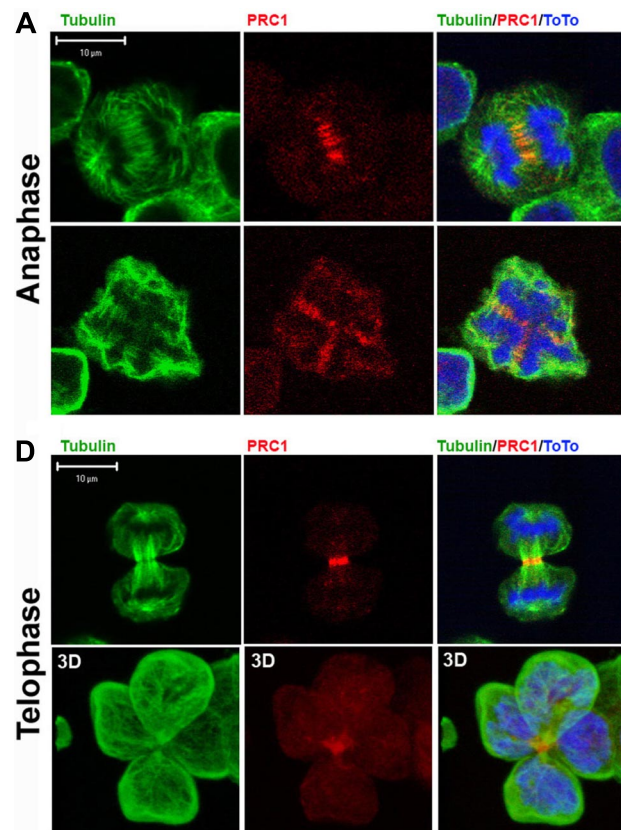

Figure 2. PRC1 localized normally to the central spindle during endomitosis. MKs were stained for tubulin (α and β, green), PRC1 (red), and TOTO (blue). The anti-α and anti-β tubulin antibodies mark the central spindle. (A) During anaphase, microtubules congregated midway between the 2 poles of the central spindle, while PRC1 accumulated in the midzone and colocalized with the central spindle. (B) During telophase, the central spindle was highly concentrated, forming 1 intercellular bridge. PRC1 was present in the center of the central spindle.

Nonmuscle myosin IIA (hereafter called myosin II) is the prevalent heavy chain of nonmuscle myosin II in platelets and MKs.[20-22] For mitotic and endomitotic MKs, myosin II was localized ubiquitously throughout the cytoplasm. Surprisingly, among 177 dipolar mitotic/endomitotic MKs examined from the beginning of furrow ingression to the end of telophase, only 13% showed a clear but weak accumulation of myosin II around the furrow cleavage; 13% showed a very weak signal at the threshold of detection (Figure 3A; 4 independent experiments), while the others (~74%) did not show any detectable accumulation of myosin II. When detectable, myosin II accumulation was almost only seen at late telophase. Moreover, in the 24 multipolar endomitotic MKs examined from the beginning of furrow ingression to the end of telophase, we were unable to detect a clear accumulation of myosin II, except for 4 individual MKs where a signal at the threshold of detection was seen in some parts of the cleavage furrow (Figure 3B; 4 independent experiments). In contrast, an obvious accumulation of myosin II in the midzone (anaphase) or in the midbody (telophase) was clearly seen by immunofluorescence in mitosis of the monoblastic U937 cells (Figure 3C) and of primary erythroblasts undergoing differentiation (data not shown). The myosin II fluorescence intensity ratio between the midzone cortex and cytoplasm was quantified by Image J. For dipolar telophase MKs (n = 11), the ratio was 1.45, and for U937 (n = 13) this ratio increased to 2.41 (P < .001). These results point out a main defect in the formation of the contractile ring in MKs endomitosis, even when a furrow ingression is present, and show
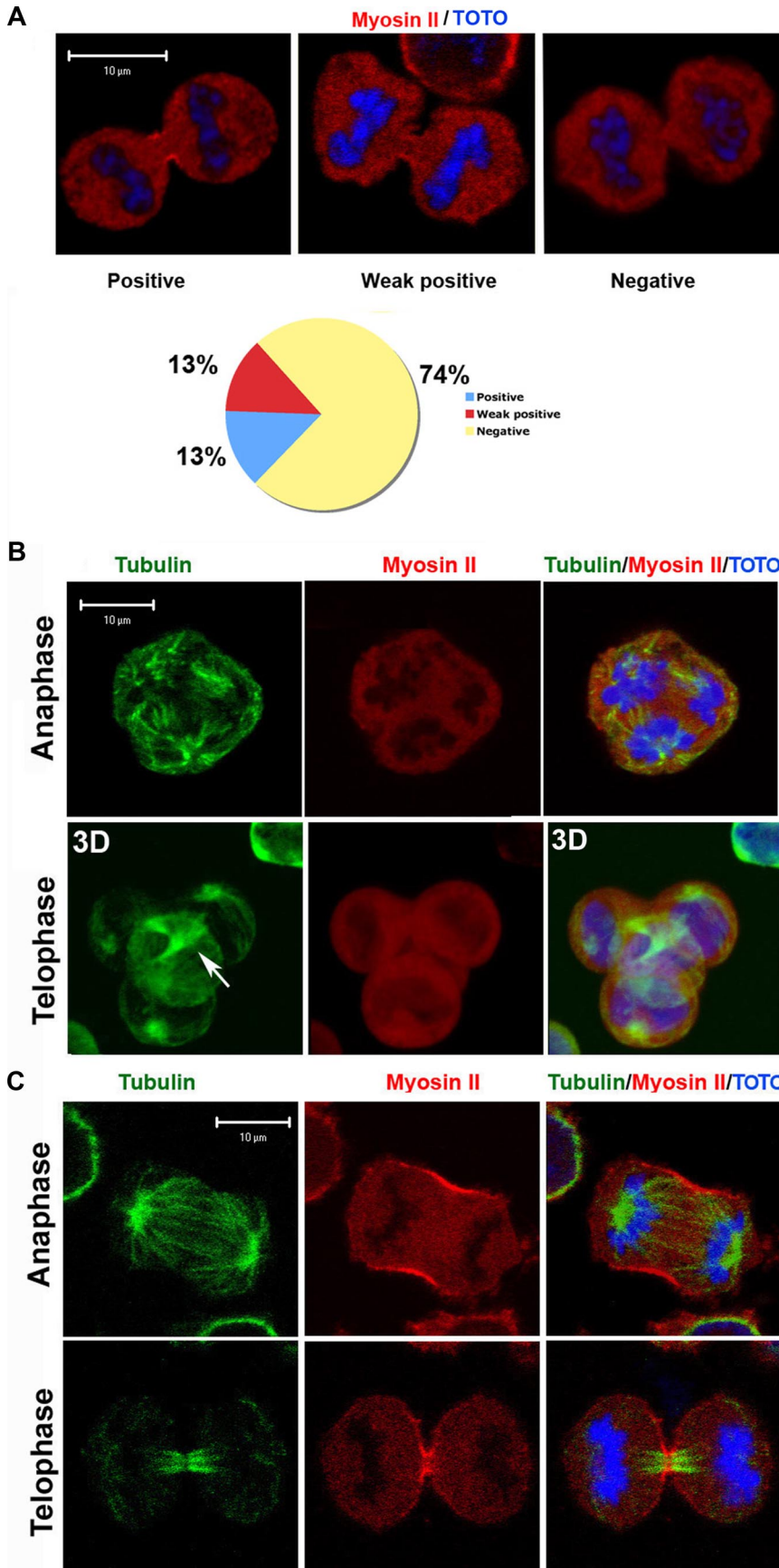
Figure 3. Absence of nonmuscle myosin IIA accumulation in the contractile ring during MK mitosis or endomitosis. Cells were stained for tubulin (α and β, green) and nonmuscle myosin IIA (red). DNA was stained with TOTO (blue). (A) Only 13% of dipolar mitotic/endomitotic MKs showed a clear accumulation of myosin II at the midzone or in the midbody, 13% showed either a signal at the threshold of detection or an incomplete accumulation at one part of the furrow, and 74% were negative. (B) Myosin II accumulation was not observed in the midzone or in the midbody of multipolar endomitosis. arrow indicates the location of midbody. (C) Myosin II accumulation was clearly detected in the midzone and the midbody of control U937 cells in mitosis.

Figure 4. Accumulation of F-actin in the contractile ring is incomplete during MK endomitosis. MKs were stained for F-actin (phalloidin-TRITC, red) or tubulin (green) and TOTO (blue). (A) F-actin accumulation around the midzone at the site of furrow ingression in dipolar mitotic/endomitotic MKs (i,ii). Incomplete F-actin accumulation (arrows) at the site of furrow ingression in multipolar endomitotic MKs (iii,iv). (B) In multipolar endomitosis, accumulation of F-actin was seen at only some parts of midzone where a local ingression is seen (arrows). (C,D) Rho inhibition by TatC3 prevents F-actin accumulation (C) and RhoA localization (D) in the midzone and spindle elongation.
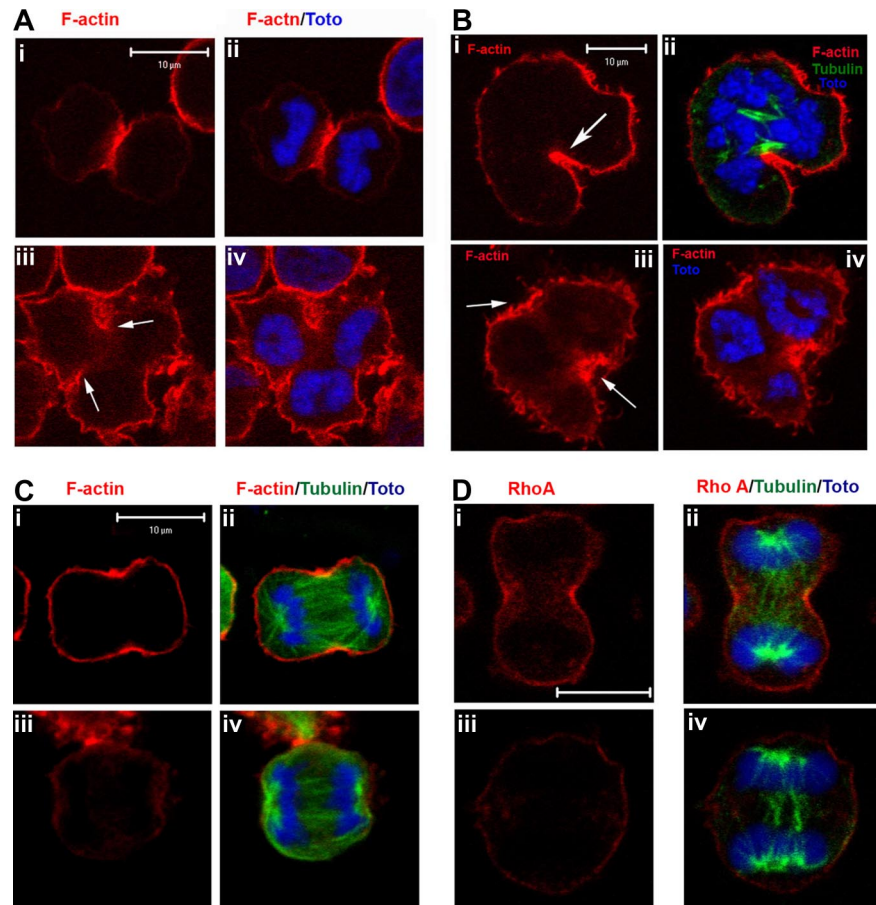
that MKs with a "normal" bipolar spindle were heterogeneous concerning myosin II accumulation at the cleavage furrow.

F-actin accumulation is incomplete in the contractile ring of endomitotic MKs

We also studied another principal component of the contractile ring, F-actin. For dipolar mitotic or endomitotic MKs, an accumulation of actin filaments appearing as a band of fluorescence around the midzone was clearly observed at the site of furrow ingression (Figure 4Ai,ii). One hundred eighty nine dipolar mitotic/endomitotic cells from the beginning of furrowing to the end of cytokinesis were examined in 3 independent experiments. All cells displayed an F-actin ring around the midzone or the midbody cortex.

For multipolar endomitotic MKs (4N to 8N or > 8N), F-actin accumulation appeared to be incomplete at the cleavage furrow (Figure 4Aiii,iv;Bi-iv). Interestingly, F-actin accumulation on a part of the furrow correlated with its local ingression (Figure 4Bi-iv).

Rho A is localized to some extent at the cleavage furrow in endomitotic MKs

The RhoA pathway is a central player in the assembly of the contractile ring during cytokinesis. Activated RhoA could regulate actin polymerization and myosin activation at the midzone through interactions with different effectors.[9] We thus examined RhoA localization during CD41+ MK mitosis and endomitosis. For dipolar MKs, RhoA was concentrated in the midzone cortex during anaphase or on the cleavage furrow during telophase (Figure 5Ai,ii; Bi,ii). For multipolar endomitotic MKs, no evident accumulation of RhoA in the midzone cortex was seen during anaphase

(Figure 5Aiii,iv). However, during telophase or reversal of cytokinesis, RhoA was usually and incompletely concentrated in the cleavage furrow (Figure 5Biii,iv arrows 1,2). Nevertheless, some MKs could be observed with a RhoA accumulation all around the cleavage furrow at the end of telophase (Figure 5Ciii,iv). In general, the cleavage furrow ingression was more pronounced at sites where RhoA was accumulated (Figure 5Ci,ii) suggesting that RhoA might be activated at some extent during endomitosis.

Rho inhibition prevents F-actin accumulation in the midzone and spindle elongation

A RhoA inhibitor (TatC3) and its control (mutated TatC3)[23] were delivered by electroporation into CD41+ MKs at day 6 of culture. We then checked the accumulation of F-actin in the midzone of dipolar mitotic/endomitotic MK cells 4 hours after electroporation (3 independent experiments). Compared with their controls (Figure 4Ci,ii;Di,ii), furrow formation and cell elongation was strongly inhibited in TatC3 treated dipolar mitotic or endomitotic MKs. Despite the formation of central spindle, there was no accumulation of F-actin in the midzone. Moreover, actin polymerization around the cell cortex was also clearly decreased (Figure 4Ciii,iv). In addition, accumulation of RhoA in the midzone could not be detected (Figure 4Diii,iv). These results suggest that Rho is not only necessary for contractile ring formation but is also implicated in spindle elongation during anaphase B.

Inhibition of Rho and Rock increases MK polyploidization

Because Rock is an important effector of RhoA during cytokinesis, we inhibited its action with Y27632. To investigate if Rho/Rock are
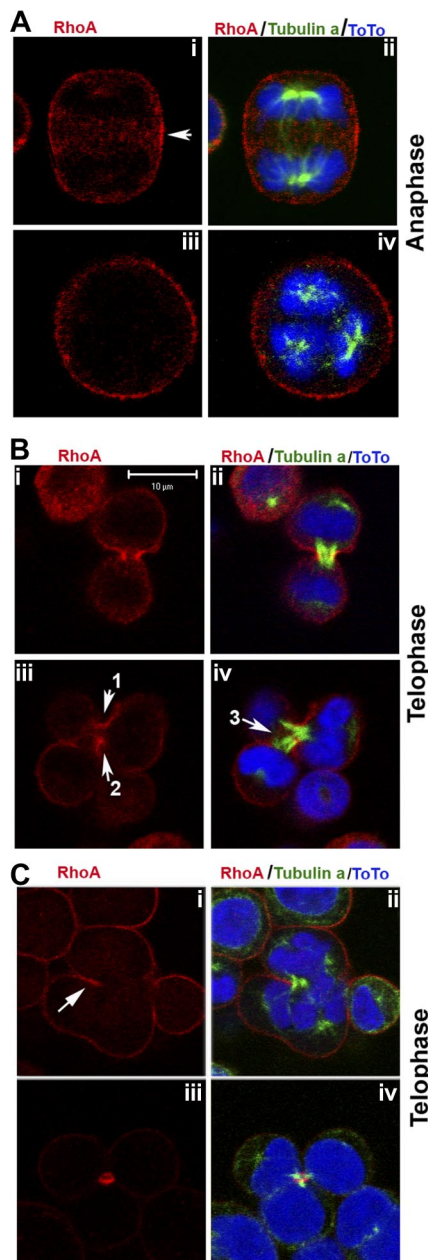
Figure 5. RhoA is localized to some extent at the cleavage furrow in endomitotic MK. Cells were stained for tubulin (α and β, green) and RhoA (red). (A) RhoA localization during anaphase. In dipolar mitotic/endomitotic MK, RhoA was concentrated around the midzone cortex (i,ii). In polyploid endomitotic MK, RhoA could not be detected in the midzone (iii,iv). (B) RhoA localization during telophase. In dipolar mitotic/endomitotic MK, RhoA was concentrated in the cleavage furrow (i,ii). In polyploid endomitotic MK, RhoA was only detected in the deepest ingressions of the cleavage furrow (iii,iv, arrows 1,2). (C) RhoA localization at the end of telophase. RhoA was localized at all sides of the cleavage furrow in dipolar mitotic/endomitotic MK (iii,iv). In multipolar endomitosis, RhoA was accumulated at only one part of the cleavage furrow and at a zone corresponding to a local ingression (indicated by arrow, i,ii).

involved in MK endomitosis, TatC3 and Y27632 were used. TatC3 and its mutated control were delivered into MKs culture by electroporation at day 5 while Y27632 was added directly at day 6. The efficiency of TatC3 delivery was evaluated to exceed 70% by studying stress fiber formation of CD41$^+$ cells (data not shown). The ploidy level of CD41$^+$/CD42$^+$ MKs was analyzed by flow cytometry 72 hours after addition of TatC3 and Y27632, respectively (Figure 6A,B). Addition of Y27632 to MKs cultures led to a significant increase in MK polyploidization because the mean

ploidy was increased from 3.68N to 6.02N (n = 3, $P < .001$). Inhibition of RhoA by TatC3 had very similar effect with an increase in the mean ploidy from 3.79N to 5.69N (n = 3, $P < .005$), suggesting that activation of the Rho/Rock pathway may play a negative role on MK polyploidization. In contrast, an inhibition of RhoA activity by TatC3 in CD41$^-$ cells has only a minor effect on polyploidization (data not shown).

A RhoA dominant negative and a Rock I shRNA increase MK polyploidization

The above results suggested that Rho/Rock activation was playing a negative role in endomitosis. However, because inhibitors may lack specificity, we used more specific inhibition approaches using a RhoA dominant negative (RhoAN19) inserted in a Moloney derived retrovirus (Migr-RhoN19-GFP) and a Rock I shRNA vectorized in an HIV-derived lentivirus. CD34$^+$ cells were infected at day 4 of culture and the ploidy level of GFP$^+$/CD41$^+$/CD42$^+$ cells was analyzed by flow cytometry at day 9 of culture. Expression of both the RhoA dominant negative and the Rock 1 shRNA moderately, but significantly, increased MK ploidy (Figure 6C-E). The mean ploidy level was increased from 2.85N (control) to 3.54N (n = 3, $P < .03$) by RhoN19 and from 3.62N (SCR shRNA) to 4.68N (n = 3, $P < .04$) by Rock I shRNA. In order to confirm that Rock I was efficiently depleted by the shRNA, the GFP$^+$ cell population was sorted 48 hours after infection. Western blot analysis revealed an approximately 40% reduction in the Rock I protein level in comparison to the scramble (SCR) shRNA used as a control. A similar reduction (35%) was found at the mRNA level by Real time RT-PCR (Figure 6D). This incomplete depletion may explain why the shRNA was less effective than the Rock inhibitor Y27362 which also inhibits Rock II efficiently.[24]

Rock inhibition by Y27632 reduces furrow ingression and spindle elongation

Our results show that inhibition of Rock by Y27632 decreased also F-actin accumulation in the midzone and actin polymerization around the cortex of dipolar mitotic or endomitotic MK (data not shown), as observed with RhoA inhibition. To check more precisely if Rock inhibition also inhibits furrowing and spindle elongation, we used real-time video microscopy to monitor endomitosis in H2B-GFP–expressing MKs treated for 12 hours with Y27632. Thirty-nine endomitotic MKs (25 treated with Y27632 and 17 without Y27632) were filmed in 3 independent experiments. Y27632-treated MKs showed an apparently normal metaphase-to-anaphase transition. However, furrow ingression was less marked than in control MKs (Figure 7; Videos S3,S4). In control cultures, 1 of the 17 endomitotic MKs examined started an early reversal of cytokinesis, that is, before the step when the daughter cells remained connected by a thin cytoplasmic bridge. This endomitotic MK had a ploidy over 8N. In contrast, in the presence of Y27632, 30% dipolar endomitosis (4 of 12) exhibited an incomplete furrowing before a reversal of cytokinesis and this ratio reached 77% in multipolar endomitosis (10 of 13) with a mean average of approximately 56% if all endomitotic MKs were considered (n = 25).

Moreover, Rock inhibition also accelerated reversal of cytokinesis. In untreated MKs, the average duration from the beginning of furrow ingression to the end of cytokinesis failure was 46.3 minutes for dipolar (n = 7) and 37.5 minutes for multipolar (n = 10) endomitotic MKs. In contrast, the process took 28.0 minutes for
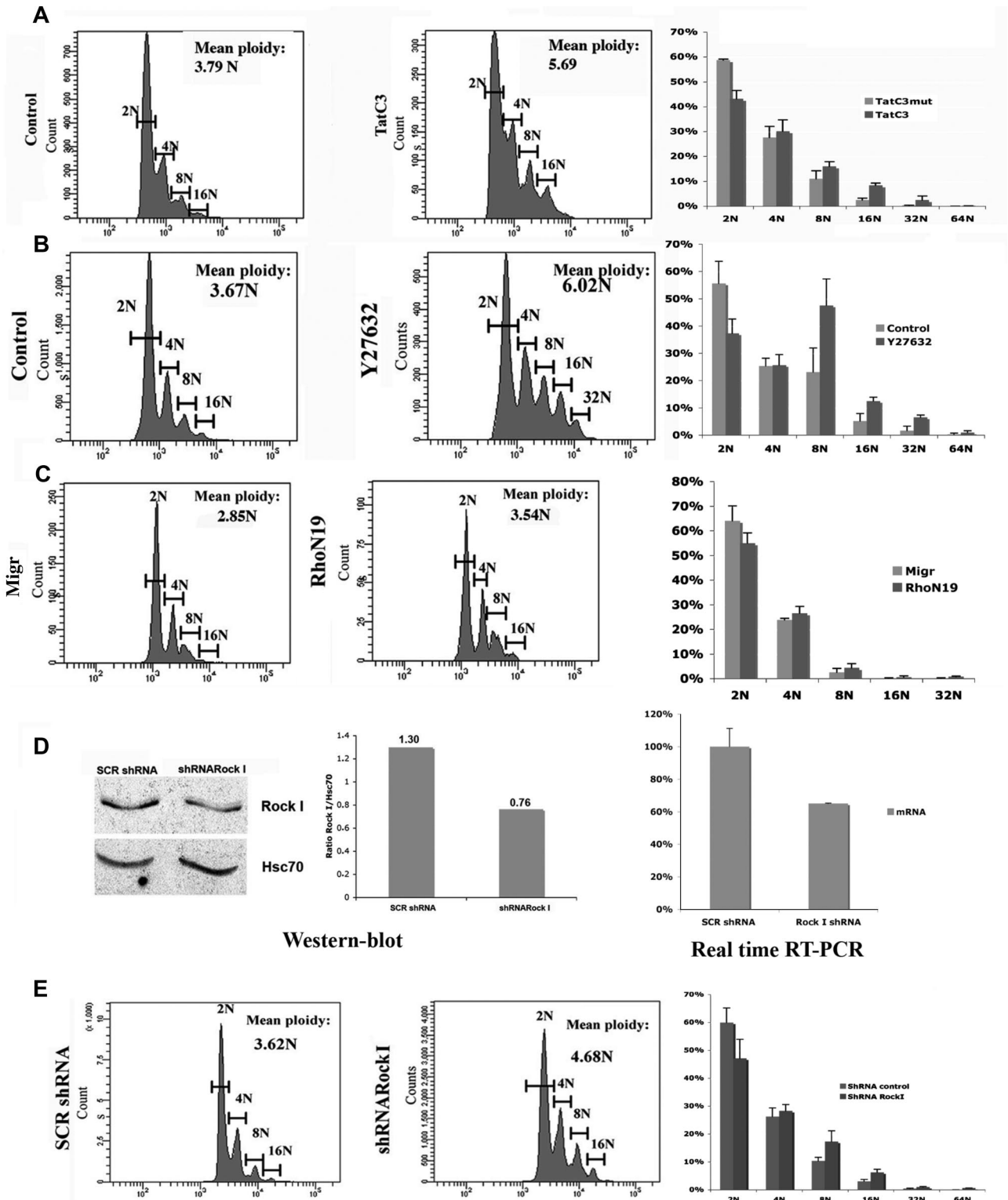
Figure 6. Effects of RhoA or Rock inhibition on MK polyploidization. (A) Effects of RhoA (TatC3) inhibitors on MK polyploidization. The ploidy level of CD41$^+$/CD42$^+$ MKs was analyzed at day 8 or 9 of culture (72 hours after addition of the inhibitors). The mean ploidy was calculated from the number of cells of each ploidy class in 3 independent experiments. Mean ploidy levels was 3.79N in the control and 5.69N with TatC3 (n = 3, $P <$ .005). The ploidy histograms are illustrated on the right part of the figure. (B) Effects of Rock (Y27632) inhibitor on MK polyploidization. The mean ploidy levels was 3.67N in the control and 6.02N with Y27632 (n = 3, $P <$ .001). (C) Effect of a RhoA dominant negative (RhoA N19) on MK polyploidization. The ploidy level of GFP$^+$/CD41$^+$/CD42$^+$ cells was analyzed by flow cytometry at day 9 of culture. The mean ploidy was calculated from the number of cells in each ploidy class in 3 independent experiments. The mean ploidy level was 3.72N with RhoN19 and 3.2 N with the empty Migr (n = 3, $P <$ .03). (D) The effect of Rock I shRNA was ascertained by Western blotting and real time RT-PCR. Western blot quantification showing that the protein levels of Rock I/Hsc70 (used as a control of protein loading) was reduced approximately 40% by the specific Rock I shRNA compared with the SCR shRNA (control). Real-time RT-PCR showing that the mRNA level of Rock I mRNA was reduced approximately 35% by the specific Rock I shRNA compared with SCR shRNA (control). (E) Effect of a Rock I shRNA on MK polyploidization. The mean ploidy level was analyzed as described above: SCR shRNA control (3.62N); Rock I shRNA (4.68N; n = 3, $P <$ .04).
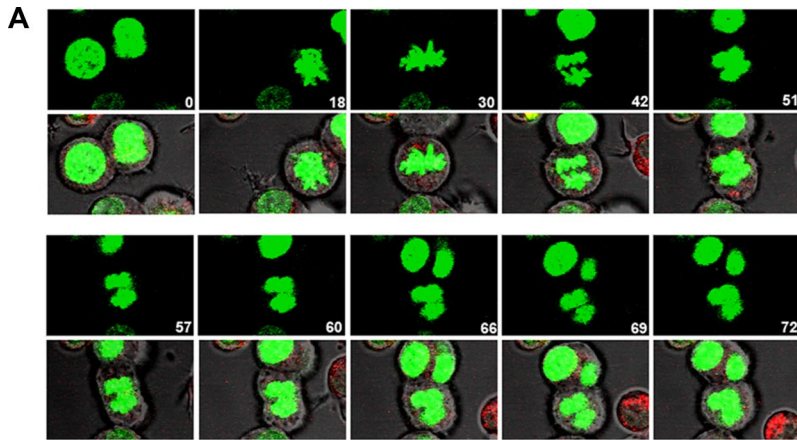
Figure 7. Inhibition of Rock by Y27632 reduces furrow ingression. MKs transduced with H2B-GFP were treated for 12 hours with Y27632 and then filmed by real-time video microscopy. Cells were stained with CellTracker Red and serial images were obtained at 3-minute intervals. Timing (min) relative to the first image is indicated. (A) Diploid endomitosis of MK treated with Y27632 proceeded generally as a normal endomitosis, but with a reduced cell elongation (see also panel C) and less evident cleavage furrow formation. (B) Polyploid endomitosis of MK treated with Y27632 showing less cleavage furrow formation (images 21-36). These time-lapse images are available in Videos S3 and S4. (C) The distance between 2 centers of separating nuclear masses in mitosis and dipolar endomitosis was measured at end of telophase of Y27632-treated and untreated MK. In untreated MK (Control), the average distance reduced approximately 16% during endomitosis compared with mitosis. For Y27632-treated MKs, the average inter-nuclear distance of dipolar endomitosis was continually decreased approximately 20% compared with untreated MK.
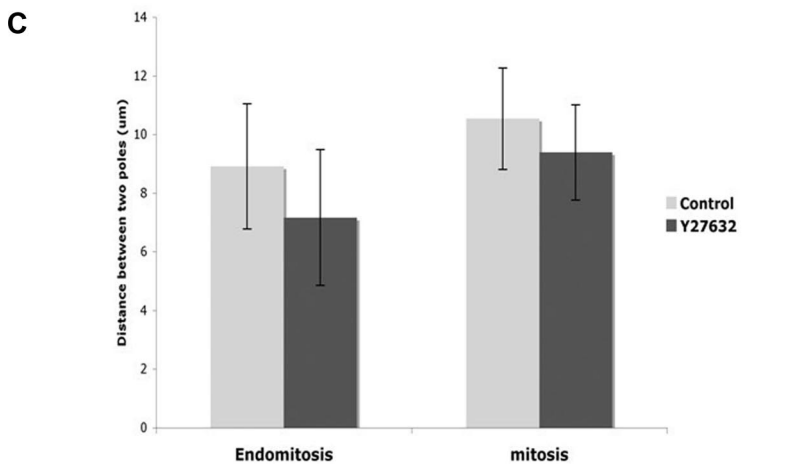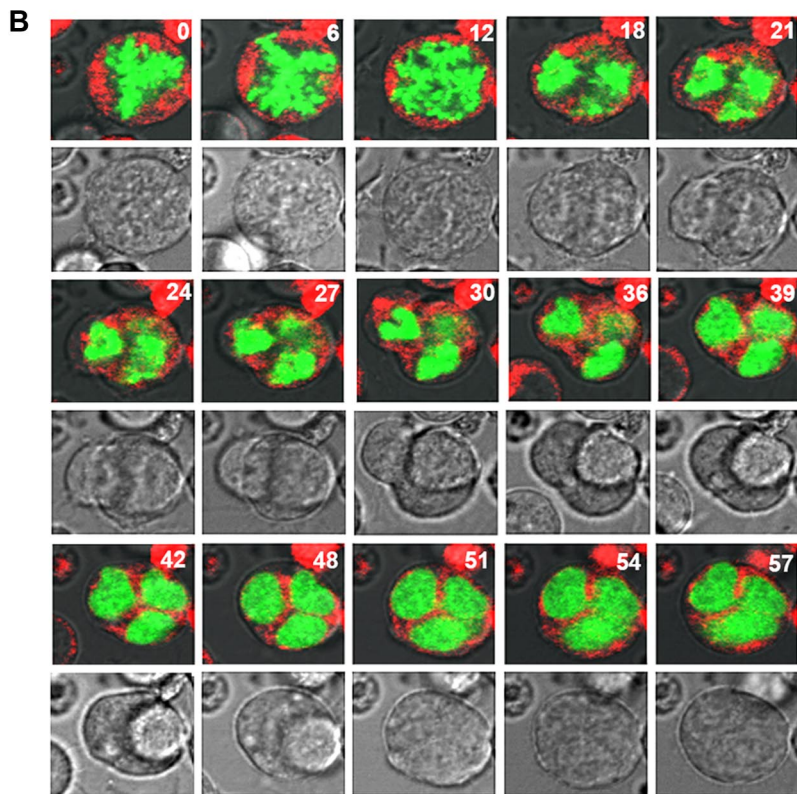
dipolar (n = 12) and 23.3 minutes for multipolar (n = 13) Y27632-treated endomitotic MKs. Interestingly, for dipolar endomitosis, Rock inhibition also decreased the average internuclear distance at the end of telophase (before the beginning of the reversal of cytokinesis) approximately 20% (n = 28 with Y27632, n = 35 for control, $P < .001$; Figure 7C).

In conclusion, these data indicate that Rock inhibition markedly impairs furrowing in endomitotic MKs and decreases the cell elongation and duration of the cytokinesis and the reversal of cytokinesis (almost 40%, $P < .05$).

Discussion

During differentiation, immature MKs increase their ploidy by endomitosis to augment their size. Among mammalian cells, MK is the unique cell type in which polyploidization is an intrinsic part of the differentiation process. Some other cells may become polyploid, but only in response to certain stimuli such as a functional stress or senescence.[25] The molecular mechanism of MK endomitosis remains poorly understood. Several studies have suggested that MK endomitosis proceeds like a normal mitosis till anaphase A but aborts at this stage because later phases of the mitosis, including anaphase B, were not observed.[1,2] Here, we used H2B-GFP on imaged living human MKs to describe more precisely the process of MK endomitosis. Our results clearly show that anaphase and telophase occur during MK endomitosis. Furthermore, cells begin cytokinesis with a nearly complete furrow completion between the 2N and 4N stages, but the process arrests. Then, the 2 daughter cells that remain joined by a thin cytoplasm bridge undergo a backward movement to ultimately reunify in one 4N cell with only 1 or 2 nuclear masses. This demonstrates that the main defect is the failure of abcission. A similar, but more complex process was observed in MK with higher ploidy undergoing endomitosis because a partial furrow ingression was observed. With the use of a similar approach and primary murine MKs expressing YFP-tubulin, Geddis et al have recently reported that polyploidization corresponded to a failure of late cytokinesis associated with furrow regression.[6] Both results are in overall in agreement except that the timing of endomitotic process from anaphase to reversal of cytokinesis was twice longer in human MKs (around 40 min vs 20 min in mouse). Thus, video microscopy of living primary MKs used in combination with different GFP fusion proteins provides a powerful approach to understand the precise mechanism of MK polyploidization.

To understand why cytokinesis cannot fully accomplish during MK endomitosis, we examined the central machine for cell division.[3,4] The presence of a normal central spindle in endomitosis has been a subject of controversy, especially for the presence and localization of Aurora B and Survivin.[26,27] Our results show that the central spindle was almost correctly assembled during endomitosis with the presence of its main components: chromosome passenger proteins such as Survivin and Aurora B (data not shown), the central spindling complex and the microtubule associated protein PRC1. Thus, the cytokinesis failure in MKs does not seem to be related to a defect in the central spindle. These data concord with the fact that furrow formation localized normally at the equatorial plate in diploid endomitotic MKs.

In contrast, we observed a major defect in the contractile ring. In dipolar mitosis or dipolar endomitosis, F-actin accumulated in the midzone, but not myosin II. In multipolar endomitosis, less F-actin and no myosin II were concentrated especially in the midzone. In animal cells, a contractile ring is generally formed to induce the cleavage between the 2 daughter cells at the end of cytokinesis. However, the contractile ring may be dispensable for both furrow formation and cytokinesis. For example, some adherent animal cells undergo cytokinesis without apparent concentration of F-actin and myosin II in the furrow.[28] Similarly, myosin II–null *Dictyostelium* cells form a cleavage furrow in the equatorial region and divide efficiently on a substrate. In contrast, non adherent cells with a disruption of myosin II function cannot undergo cytokinesis.[29] In MKs the defect in myosin II accumulation markedly decreases the constriction forces of the actomyosin ring and may also modify the actin turn over. The polar traction forces are potentially sufficient to induce furrow formation, but the decrease of constricting forces probably causes this failure of cytokinesis. The daughter cells remain thus connected by a cytoplasm bridge for a certain moment under the polar traction forces. However, these forces cannot counterbalance the centripetal forces and the daughter cells reunify by a backward movement. This model is similar to that described for other nonadherent cells without contractile ring formation which form a cleavage furrow but are unable to complete cytokinesis.[28,30]

The Rho/Rock pathway plays a major role in cytokinesis by regulating actin polymerization and myosin II activity at the cleavage furrow.[4,8,9] First, activated RhoA can directly control actin polymerization at the midzone by the formin-profilin machine. Second, RhoA can activate Rock and Citron kinase which in turn regulate myosin II activation by MLC2 (myosin light chain 2) phosphorylation. At the same time, activated Rock can also increase actin polymerization by activating LIMK which subsequently increases cofilin phosphorylation.[31]

Our results also suggest that the endomitotic process is not related to an absence, but to a decrease of RhoA activity. Several evidences support this hypothesis. First, we show that RhoA was localized at the cleavage furrow during a 2N to 4N endomitosis. In higher ploidy endomitotic MKs, Rho A was concentrated together with F-actin at the level of ingression, but not all around the cleavage furrow. A more complete inhibition of RhoA activity by TatC3 led to an absence of RhoA and actin accumulation at the midzone. This suggests that the accumulation of F-actin in the midzone directly correlates with the presence of RhoA and that RhoA is only partially activated in the midzone or on the cleavage furrow in polyploid MKs. Furthermore, RhoA inhibition induced an absence of contractile ring leading to an increase in MK polyploidization. Second, the spindle elongation was decreased of approximately 16% in endomitotic 2N to 4N MKs in comparison to mitotic MKs. Inhibition of Rho activity by TatC3 inhibited strongly spindle elongation. This further suggests that some Rho activity must remain in endomitotic MKs to allow spindle elongation.

In Drosophila, it has been demonstrated that Rock I activity is required for anaphase cell elongation and that elongation seems essential for complete furrow formation.[10] Inhibition of Rock by Y27632 decreased anaphase elongation of MK. We observed also that inhibition of Rock had an even more pronounced effect than inhibition of RhoA in MK polyploidization. This further suggests that Rock activation plays a crucial role in MK polyploidization.

Our results suggest that the switch during MK differentiation from mitosis to endomitosis at the 2N stage is related to an

incomplete RhoA activation, which leads to a defect in contractile ring and spindle elongation. At higher stages of ploidy, the formation of a complex and short spindle increases the microtubule density which, in association with a more complete defect in RhoA local activation, further inhibits furrow formation. The precise mechanism responsible of the defect in RhoA local activation and the absence of myosin II in MK contractile ring remains to be determined, but this mechanism might be regulated by a lineage specific process. In human cells, the central-spindle-associated RhoGEF (ECT2) and GAP (MgcRacGAP) interact and promote RhoA accumulation and activation in the midzone. The depletion of ECT2 or MgcRacGAP blocked RhoA activation and both myosin II and F-actin accumulation in the contractile ring.[8] The work of Geddis et al has shown that MgcRacGAP is located normally in the midzone during anaphase of endomitosis.[5] Overexpression of an active form of RhoA (RhoV14) in MKs did not change MK ploidy level (data not shown). This suggests that the impaired mechanisms in MKs are the localization and concentration of RhoA in the midzone. Thus, it will be important to check if ECT2 and its regulators (Polo like kinase 1 or kinesin-6) accumulate in the midzone of MKs and function to recruit and activate RhoA locally.[8,11,32]

In conclusion, our data highlight a new mechanism of cytokinesis failure in mammalian cell, which is related to the defect in contractile ring and in the Rho/Rock pathway. This study offers new avenue for investigation on the precise mechanism of cytokinesis failure and polyploidization in MKs.

Authorship

Contribution: L.L. designed and performed experiments, analyzed data, and critically read the paper; A.J. performed experiments and analyzed data; F.A. and J.L. performed experiments; F.L. performed sorting experiments; N.D. designed and performed experiments; W.V. designed the work, supervised the experiments, and wrote the paper; and Y.C. designed the work, designed and performed experiments, analyzed data, and wrote the paper.

Conflict-of-interest disclosure: The authors declare no competing financial interests.

Correspondence: William Vainchenker, Inserm, U790, Hématopoïèse et Cellules Souches Normales et Pathologiques Institut Gustave Roussy, 39 Rue Camille Desmoulins, 94805 Villejuif cedex, France; e-mail: verpre@igr.fr.

References

1. Nagata Y, Muro Y, Todokoro K. Thrombopoietin-induced polyploidization of bone marrow megakaryocytes is due to a unique regulatory mechanism in late mitosis. J Cell Biol. 1997;139:449-457.

2. Vitrat N, Cohen-Solal K, Pique C, et al. Endomitosis of human megakaryocytes are due to abortive mitosis. Blood. 1998;91:3711-3723.

3. Bowerman B. Cell division: timing the machine. Nature. 2004;430:840-842.

4. Glotzer M. The molecular requirements for cytokinesis. Science. 2005;307:1735-1739.

5. Geddis AE, Kaushansky K. Endomitotic megakaryocytes form a midzone in anaphase but have a deficiency in cleavage furrow formation. Cell Cycle. 2006;5:538-545.

6. Geddis AE, Fox NE, Tkachenko E, Kaushansky K. Endomitotic megakaryocytes that form a bipolar spindle exhibit cleavage furrow ingression followed by furrow regression. Cell Cycle. 2007;6:455-460.

7. Jaffe AB, Hall A. Rho GTPases: biochemistry and biology. Annu Rev Cell Dev Biol. 2005;21:247-269.

8. Wadsworth P. Cytokinesis: Rho marks the spot. Curr Biol. 2005;15:R871-874.

9. Piekny A, Werner M, Glotzer M, et al. Cytokinesis: welcome to the Rho zone. Trends Cell Biol. 2005;15:651-658.

10. Petronczki, M, Glotzer, M, Kraut N, Peters, JM Polo-like kinase 1 triggers the initiation of cytokinesis in human cells by promoting recruitment of the RhoGEF Ect2 to the central spindle. Dev Cell. 2007;12:713-725.

11. Hickson GR, Echard A, O'Farrell PH. Rho-kinase controls cell shape changes during cytokinesis. Curr Biol. 2006;16:359-370.

12. Norol F, Vitrat N, Cramer E, et al. Effects of cytokines on platelet production from blood and marrow CD34+ cells. Blood. 1998;91:830-843.

13. Abbas-Terki T, Blanco-Bose W, Deglon N, Pralong W, Aebischer P. Lentiviral-mediated RNA interference. Hum Gene Ther. 2002;13:2197-2201.

14. Brummelkamp TR, Bernards R, Agami R. A system for stable expression of short interfering RNAs in mammalian cells. Science. 2002;296:550-553.

15. Naldini L, Blomer U, Gallay P, et al. In vivo gene delivery and stable transduction of nondividing cells by a lentiviral vector. Science. 1996;272:263-267.

16. Chang Y, Aurade F, Larbret F, et al. Proplatelet formation is regulated by the Rho/ROCK pathway. Blood. 2007;109:4229-4236.

17. Zhang Y, Wittner M, Bouamar, H, et al. Identification of CXCR4 as a new nitric oxide-regulated gene in human CD34+ cells. Stem Cells. 2007;25:211-219.

18. Lens SM, Vader G, Medema RH. The case for Survivin as mitotic regulator. Curr Opin Cell Biol. 2006;18:616-622.

19. Mollinari C, Kleman JP, Jiang W, Schoehn G, Hunter T, Margolis RL. PRC1 is a microtubule binding and bundling protein essential to maintain the mitotic spindle midzone. J Cell Biol. 2002;157:1175-1186.

20. Maupin P, Phillips CL, Adelstein RS, Pollard TD. Differential localization of myosin-II isozymes in human cultured cells and blood cells. J Cell Sci. 1994;107(Pt 11):3077-3090.

21. Kawamoto S, Adelstein RS. Chicken nonmuscle myosin heavy chains: differential expression of two mRNAs and evidence for two different polypeptides. J Cell Biol. 1991;112:915-924.

22. Sellers JR. Myosins: a diverse superfamily. Biochim Biophys Acta. 2000;1496:3-22.

23. Sebbagh M, Renvoize C, Hamelin J, Riche N, Bertoglio J, Breard J. Caspase-3-mediated cleavage of ROCK I induces MLC phosphorylation and apoptotic membrane blebbing. Nat Cell Biol. 2001;3:346-352.

24. Ishizaki T, Uehata M, Tamechika I, et al. Pharmacological properties of Y-27632, a specific inhibitor of rho-associated kinases. Mol Pharmacol. 2000;57:976-983.

25. Zimmet J, Ravid K. Polyploidy: occurrence in nature, mechanisms, and significance for the megakaryocyte-platelet system. Exp Hematol. 2000;28:3-16.

26. Zhang Y, Nagata Y, Yu G, et al. Aberrant quantity and localization of Aurora-B/AIM-1 and survivin during megakaryocyte polyploidization and the consequences of Aurora-B/AIM-1-deregulated expression. Blood. 2004;103:3717-3726.

27. Geddis AE, Kaushansky K. Megakaryocytes express functional Aurora-B kinase in endomitosis. Blood. 2004;104:1017-1024.

28. O'Connell CB, Wheatley SP, Ahmed S, Wang YL. The small GTP-binding protein rho regulates cortical activities in cultured cells during division. J Cell Biol. 1999;144:305-313.

29. Uyeda TQ, Nagasaki A. Variations on a theme: the many modes of cytokinesis. Curr Opin Cell Biol. 2004;16:55-60.

30. Neujahr R, Heizer C, Gerisch G. Myosin II-independent processes in mitotic cells of Dictyostelium discoideum: redistribution of the nuclei, re-arrangement of the actin system and formation of the cleavage furrow. J Cell Sci. 1997;110(Pt 2):123-137.

31. Bernard O. Lim kinases, regulators of actin dynamics. Int J Biochem Cell Biol. 2007;39:1071-1076.

32. Burkard ME, Randall CL, Larochelle S, et al. Chemical genetics reveals the requirement for Polo-like kinase 1 activity in positioning RhoA and triggering cytokinesis in human cells. Proc Natl Acad Sci U S A. 2007;104:4383-4388.